Chemical Engineering Journal 162 (2010) 307–313

Contents lists available at ScienceDirect

Chemical Engineering Journal

journal homepage: www.elsevier.com/locate/cej

Development of a high-flame-luminosity thermophotovoltaic power system

Yueh-Heng Li[a,*], Chih-Yung Wu[b], Yung-Sheng Lien[a], Yei-Chin Chao[a,**]

[a] Department of Aeronautics and Astronautics, National Cheng Kung University, Tainan, 701, Taiwan, ROC
[b] Department of Electro-Optical Science and Engineering, Kao Yuan University, Kaohsiung County, 1821, Taiwan, ROC

ARTICLE INFO

Article history:
Received 22 February 2010
Received in revised form 24 April 2010
Accepted 28 April 2010

Keywords:
Thermophotovoltaic (TPV)
GaSb PV cells
Blended fuel
Flame luminosity

ABSTRACT

Creating high-luminescence flame is a prior consideration for the fueling system of the proposed TPV system. General methane and hydrocarbon gaseous fuels generate faint yet high-temperature flames. However, blending CH_4/CO fuel composition may lead to different flame luminescence. Depending upon the concentration ratio of CO in the CH_4/CO blended fuel mixture, flame luminescence becomes brighter, and its corresponding color turns to silver-white as the CO percentage is increased. Varied CH_4/CO blended fuel mixture has distinct laminar burning velocity functioning with equivalence ratio. Furthermore, the emissivity of flames is certainly low compared to that of solid materials, so that it is impossible to solely utilize the flame luminosity to achieve high efficiency. To ameliorate this disadvantage, a new strategy in combustor design should be comprehensively considered. Concept, design and preliminarily results of the proposed new TPV combustor are addressed.

1. Introduction

As the prevailing of mesoscale electronic devices in recent years, the demand for high-energy-density portable power supply systems becomes an urgent bottle-neck to break through. Given the high energy density of most hydrocarbon fuels compared to batteries [1], a system that effectively utilizes the fuels could potentially resolve the current hindrance. One approach to converting chemical energy of fuels into electricity in a small-scale device is to burn the fuel in cogeneration, and convert part of the energy release into electrical power by means of photovoltaics and thermoelectrics. Thermophotovoltaic (TPV) devices convert thermal radiant energy directly into electrical power, and combustion-driven TPV cogeneration systems, where the waste heat is also utilized, have found practical applications in the small-scale devices [2–5]. Since the radiant density of combustion-driven sources can be much greater than that from the sun, the electric power density of the TPV cells is much higher than that of solar cells. In general, a combustion-driven TPV power system consists of a burner/thermal sources, radiant emitter and TPV cell arrays. The overall efficiency of a combustion-driven TPV power system is ultimately related to the radiant efficiency of the emitter and the quantum efficiency of PV cells. As regards the PV cells, there are two main approaches to realizing a TPV conversion process. One uses silicon solar cells (1.1 eV). The other involves low band-gap TPV cells such as GaSb cells (0.72 eV) [6] and InGaAsSb cells (0.53 eV) [7]. Lowering the band gap of PV cells will allow more photons with lower energy to be absorbed by the PV cells and create electron–hole pairs. This is because only photons radiated by the emitter having energy greater than the band gap of PV cells can be converted into electricity. Usually, a low band-gap photovoltaic cell has high quantum efficiencies in the visible to near-infrared range, but the radiant spectrum from a conventional emitter of the combustion-driven TPV system congregates within the infrared wavelength. This spectrum mismatch leads to principle energy loss on the overall efficiency of nowadays TPV power systems. Therefore, many researchers over the world emphasize on material improvements and manufacturing development of low band-gap photovoltaic cells [6,7] and selective emitters [8,9], and on integrating spectral control devices [10] in the combustion-driven TPV power system to filter the radiant and to reflect the non-photon-convertible radiation back to the emitter.

On the other hand, flame emission spectrum mainly distributes from visible to near-infrared in wavelength, and its corresponding spectral distribution is preferable for electricity conversion via photovoltaic cells. Generally, methane and gaseous hydrocarbon fuels generate faint luminous yet high-temperature flames. However, blending of CH_4 and CO fuels may lead to much stronger flame luminosity [11]. Depending upon the fraction of CO in the CH_4/CO blended fuel mixture, flame luminosity becomes brighter, and its corresponding flame color turns into silver-white as CO percentage is increased. The high flame luminosity is induced from decomposition of metal carbonyls [12]. Carbon monoxide stored in high-pressure cylinders results in contamination from iron pen-

* Corresponding author at: IAA, National Cheng Kung University, No. 1, Ta-Hsueh Rd., Tainan, 701, Taiwan, ROC. Tel.: +886 6 2345291; fax: +886 6 2389940.
** Corresponding author at: IAA, National Cheng Kung University, No. 1, Ta-Hsueh Rd., Tainan, 701, Taiwan, ROC. Tel.: +886 6 2757575x63690; fax: +886 6 2389940.
E-mail addresses: yuehheng.li@gmail.com (Y.-H. Li), ycchao@mail.ncku.edu.tw (Y.-C. Chao).

1385-8947/$ – see front matter.
doi:10.1016/j.cej.2010.04.051

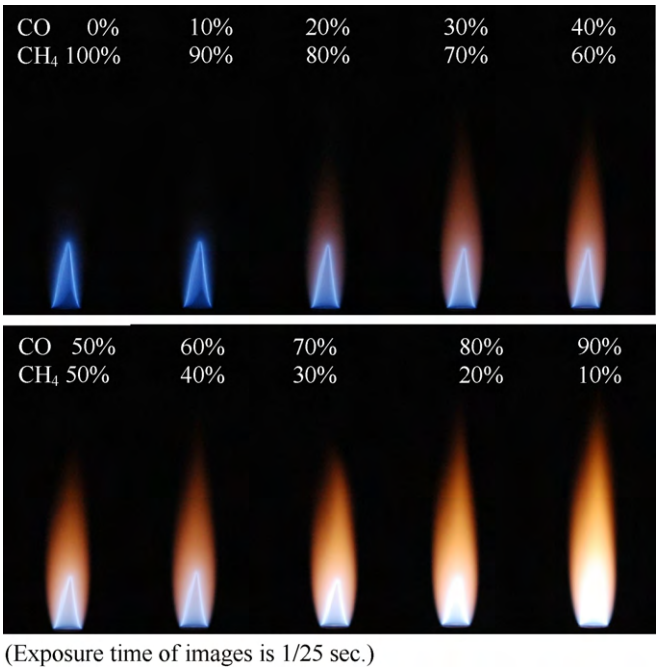

Fig. 1. Flame images in different CO/CH_4 blended fuel mixtures and fixed exit velocity of 2 m/s in a stoichiometric condition.

tacarbonyl ($Fe[CO]_5$) and, to a lesser extent, nickel tetracarbonyl ($Ni[CO]_4$) as CO reacts with the iron content in the cylinder wall. Even the process of producing CO, through steam reforming of natural gas or coal gasification, typically results in contamination by carbonyls. In addition, the unintended addition of iron pentacarbonyl to CO-fueled flame system may affect flame ignition and extinction. Addition of 50 ppm iron pentacarbonyl reduces the flame speed of stoichiometric methane–air flame by 20% [13], but addition of iron pentacarbonyl to the fuel side of a methane/air diffusion flame has no influence on the extinction strain rate [14].

In fact, the flame emissivity is very low compared to that of solid materials. It is impossible to solely utilize flame luminosity to achieve high conversion efficiency. In this paper, the novel idea of combining the visible wavelength radiation from the flame and the near-infrared wavelength radiation from the emitter is proposed to enhance the overall efficiency. The high flame luminosity from CO blended fuels is considered. When burning carbonyl-contaminated fuels, massive iron and nickel oxides will be formed and adhered on the combustion wall. The red oxide deposit often reduces the transmitted light intensity through the transparent combustor wall, or clogs in the pathway of the combustion system. Consequently, protection from deposit of metal oxides becomes an important issue in the design of a flame-luminosity thermophotovoltaic power system. A novel strategy in combustor design should be comprehensively considered. Concept, design and test results of the proposed new TPV combustor are addressed in the following sections.

2. Concept and design

2.1. Motivation and concept

In general, flame luminescence is dependent on fuel types and combustion conditions. In order to examine the effect of fuel composition on the characteristics of flame luminosity, attention is focused on stoichiometric CH_4/CO/air flame. Fig. 1 shows the photographs of the premixed stoichiometric CH_4/CO/air flame images of various CO volumetric contents in the methane–air mixtures

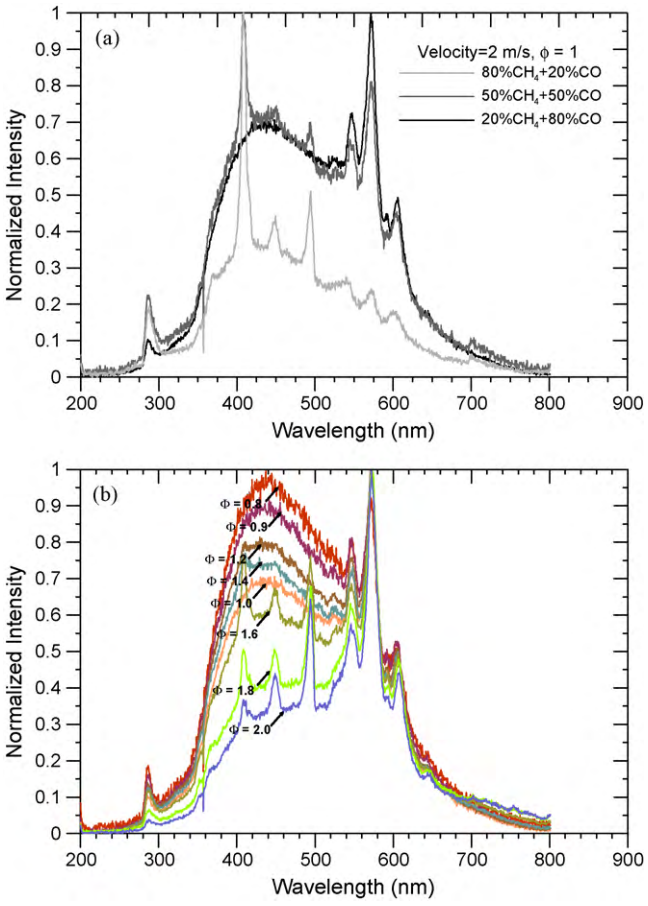

Fig. 2. Flame emission spectra in (a) different fuel blended conditions and (b) different equivalence ratios of $20\%CH_4 + 80\%CO$ case.

with a fixed flow velocity of 2.0 m/s. Each exposure time of the photographs is fixed at 1/25 s. It appears that the flame is faint-blue in color for pure methane. When 20 vol.% of CO is added to the fuel, the post-flame zone immediately becomes orange in color. The flame emission becomes bright silver-white in color as the CO concentration is increased to 70% in volume, as shown in Fig. 1. (For interpretation of the references to color in the text, the reader is referred to the web version of this article.) The emission spectrum of three typical premixed stoichiometric CH_4/CO/air flames, $80\%CH_4 + 20\%CO$, $50\%CH_4 + 50\%CO$ and $20\%CH_4 + 80\%CO$, is experimentally tested by using a monochromator combining with an ICCD camera and investigated in Fig. 2(a). There are pronounced peaks in some specific wavelengths as well as broadband underlying emissions in the three cases. The broadband emission extends throughout the visible wavelength region and varies with the equivalence ratio. Nevertheless, in the high CO percentage case ($80\%CO + 20\%CH_4$), the flame emission spectrum has a higher base broadband as compared to high methane percentage case ($20\%CO + 80\%CH_4$). The high CO percentage flame can effectively provide high intensity emission in visible wavelength for a combustion-driven TPV power system. However, the radiation from the post-flame especially for the cases with higher CO composition is induced from decomposition of metal carbonyls. It is important to note the increase in visible wavelength is related to the decrease of equivalence ratio in the case of $80\%CO + 20\%CH_4$, as shown in Fig. 2(b). Sendroy et al. [15] reported a mean iron pentacarbonyl concentration of 184 ppm in pressurized CO cylinders. However, metal carbonyls combustion will correspondingly generate metal oxide particles in product gas, and these metal oxide

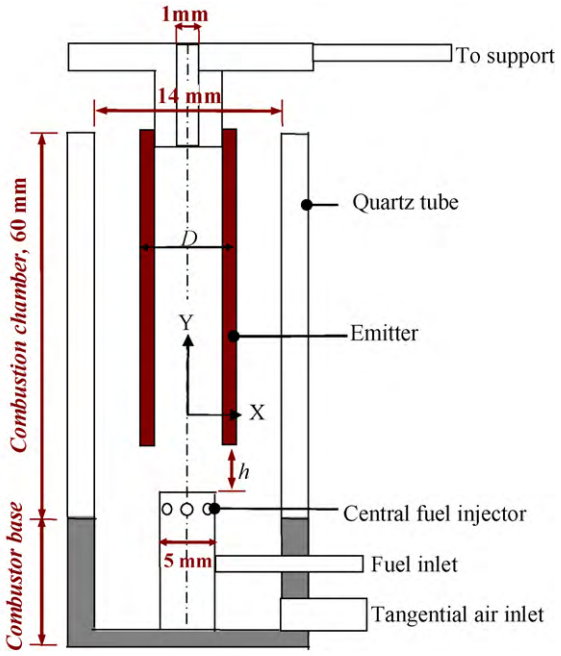

Fig. 3. Sketched diagram of the combustor.

particles are responsible for releasing visible wavelength radiation.

2.2. Design of the combustor

The design concept of this mesoscale high-luminescent-flame TPV power system is to integrate visible radiation from flames with near-infrared radiation from an emitter, and simultaneously convert these radiations into electricity via PV cells. Collecting both the flame luminosity and the thermal radiation from an emitter simultaneously in the TPV system is an efficient manner to amend the drawback of inherently low flame emissivity. Based upon this concept, a novel tube-in-the-combustor design is proposed. Fig. 3 sketches the diagram of the proposed combustor. The proposed miniature combustor can be categorized by two sections, the combustor base and the combustion chamber respectively. In the combustor base, a cylindrical tube is utilized to induce the swirling flow. The swirling flow is expected to enhance the residence time as well as fuel/air mixing, and to avoid metal oxide particles adhering to the chamber wall. Air is supplied from a compressor system, whereas methane and carbon monoxide are supplied from high-pressure gas cylinders. Separate air and fuel injecting systems are adopted in this proposed combustor. For attaining adequate and quick fuel/air mixing, blended fuels are injected radially into the main combustor through the central fuel injector to mix with oncoming swirling air flow. The fuel/air injection system inherits the flow structure characteristics of the asymmetrical combustor [16] and its advantage is to efficiently enhance the fuel/air mixing and shorten the flame length, especially in a confined and localized system. As regards the main combustion chamber section, there are the two components in the proposed combustor. One is the thermo-infrared tube serving as an emitter, and the other is a transparent tube with an overall length of 60 mm for visualization and allowing emission to PV cells. The infrared thermal tube made by silicon carbide is a typical broadband emitter and the spectrum of broadband emitters generally operates in the temperature range of about 900–1400 K. In addition, emitters have low thermal conductivities, and the radiation intensity of the emitter is proportional to its surface temperature. Accordingly, a fully aerated flame burning close to the emitter surface that heats the surface to incandescence is necessary. Certain configurations and dimensions in the combustor have to be particularly considered. For instance, the dimension of thermo-infrared tube should correlate with the space between the main combustion chamber and the thermal-infrared tube, and the flame structure and its corresponding stabilization are subject to this space in the combustor. There are three kinds of tube sizes tested in the experiments (labeled D in Fig. 3), 8, 9 and 10 mm respectively. Besides, the distance h labeled in Fig. 3 between the central fuel injector and the thermo-infrared tube is the other essential parameter in designing the miniature combustor, and there are four values on h considered in the experiments, 5, 10, 15 and 20 mm respectively.

Choosing a proper photovoltaic cell array is essential in the design of a mesoscale TPV power device. Silicon solar cells have good quantum efficiency in the 300–1200 nm wavelength, while GaSb PV cells have good quantum efficiency in the 400–1800 nm wavelength. To spectrally match the emitter radiation necessitates the use of low band GaSb TPV cells in order to simultaneously maximize both the efficiency and the power density. GaSb PV cells, fabricated by JX Crystals Inc., USA, were connected electronically in series surrounding the emitter. These cells are of backside contact type. Because only planar GaSb cells can be fabricated, it is composed of four cell arrays. Each cell array has an area of 18 cm^2 and contains two strings of six series connected cells in parallel.

2.3. Instrumentation

Various control and measuring devices, including IR thermometer, powermeter, monochromator combining with an intensified CCD (ICCD) camera, and voltage/current analyzer were used in the experiments. The IR thermometer was used to monitor the surface temperature of the emitter. The radiant intensity of flame luminosity and emitter was detected by a powermeter which has a uniform quantum efficiency ranging from ultraviolet (190 nm) to near-infrared (1100 nm). The monochromator combined with an ICCD is used to examine the radiation spectrum of the proposed combustor. The electrical output of the cells was determined using an I–V analyzer.

3. Results and discussion

3.1. Burner combustion performance

In order to understand combustion characteristics of the blended CO/CH_4 fuels inside the combustor, volumetric percentages of fuel compositions in the blended fuel mixture are varied in this study. The adiabatic, unstrained, free propagation velocities of the laminar premixed CO/CH_4/air flames are calculated using the PREMIX code of Chemkin collection 3.5. The calculated laminar burning velocities of the premixed CH_4/CO/air flames under various CH_4/CO fuel compositions and equivalence ratios are shown in Fig. 4. Note that the laminar burning velocity is calculated based on the “dry” oxidation condition, i.e. no water vapor is present in the air. Fig. 4 shows that for a fixed fuel composition the maximum burning velocity occurs on the rich side of stoichiometry. The maximum burning velocity increases with increasing CO percentage in the fuel mixture. Comparison of the computed maximum burning velocities and laminar burning velocity of stoichiometric flame for different CO percentages in fuel is depicted in Fig. 5. The computed maximum laminar burning velocity increases monotonically with increasing CO content in the methane–air mixtures. It can be found that the calculated maximum burning velocities have the same trend with those measured by Scholte and Vaags [17]. Similarly, the computed laminar burning velocity of stoichiometric

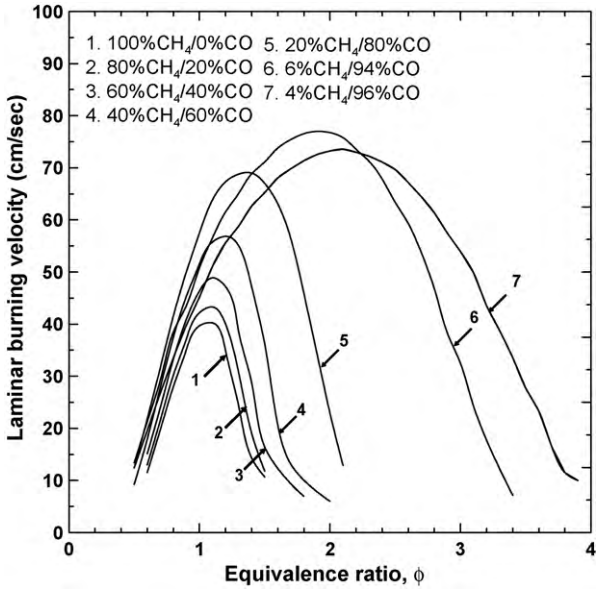

Fig. 4. Computed laminar burning velocity of the CH_4/CO/air flames as a function of equivalence ratio with various CO contents in the fuel mixture.

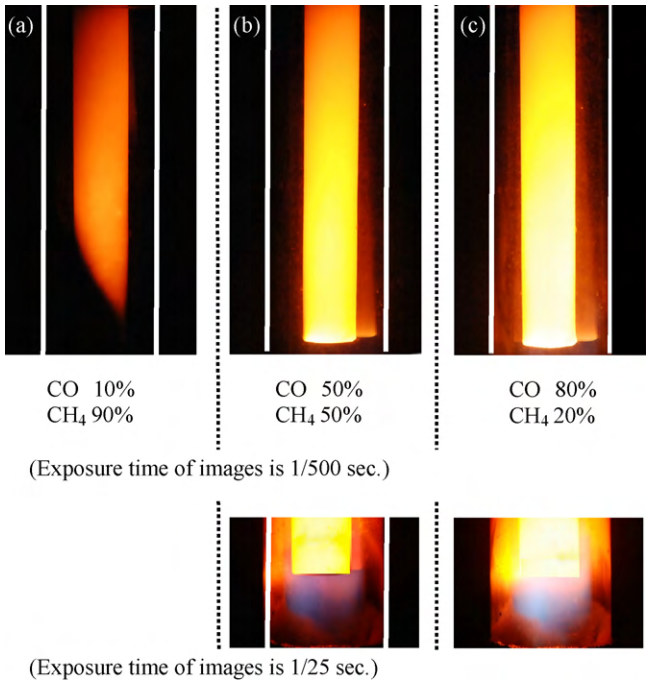

Fig. 6. Photographs of combustion phenomena in the combustor with various CO contents in the fuel mixture.

flame also increases monotonically with increasing CO percentage in the fuel mixtures, and it reaches a maximum value (57.5 m/s) at the condition of 80% of CO in fuel and then decreases rapidly as CO content is further increased. The laminar burning velocity of 20%CH_4 + 80%CO flame at stoichiometric condition is about a factor of 1.5 higher than that for pure methane flame. This fact suggests that the addition of an appropriate amount of CO to CH_4–air mixture could increase the flame propagation and influence the chemistry and structure of premixed CH_4/CO/air flames.

In order to examine the feasibility of generating stable flame luminosity and radiant emission, combustion of CH_4/CO blended fuel of stoichiometric and different fuel compositions in the combustor is performed and shown in Fig. 6. The emitter tube diameter D is 9 mm, and the distance h is fixed at 15 mm from the top of the central fuel injector. Fig. 6 displays the stable combustion phenomena inside the combustor and at the bottom end of the emitter tube in varied fuel compositions and a fixed flow velocity of 2.0 m/s, and each photograph has the same exposure time. In the case of high methane percentage fuel (90%CH_4 + 10%CO), it shows low flame luminosity and low emitter incandescence in Fig. 6(a). It appears that the flame is almost invisible at the bottom of the emitter tube. High flow velocity reduces effective heat transfer to the emitter, resulting in non-uniform and spiral-pattern emitter illumination. As the carbon monoxide concentration is increased to 50% in volume in Fig. 6(b), the blue and silver-white flame can be observed around the emitter tube at the bottom, and emitter illumination becomes more uniform and brighter compared to the previous case. Once the carbon monoxide concentration is further increased to 90% in volume in Fig. 6(c), high intensity of silver-white flame luminosity sustains and surrounds the emitter tube at the bottom. It appears that the laminar burning velocity is increasing with an increase of carbon monoxide percentage in the blended fuels. Accordingly, the flame moves upstream, successfully anchors at the bottom end of the emitter, and burns along the emitter tube. In this way, flame luminosity can efficiently integrate with emitter radiation, and enhance the radiation intensity in the visible range. In order to further verify the effect of spectral superposition, a monochromator with an ICCD is used to examine the radiation spectrum from the combustor. Fig. 7 shows the radiation spectral distribution from the silicon carbide emitter and from the flame in the proposed combustor. The broken line in Fig. 7 is the quantum efficiency of the intensifier CCD camera. The silicon carbide tube is electrical-heated and monitored by PID controller. Results indicate that the radiation from the silicon carbide is congregated in the near-infrared wavelength, as shown by the grey curve in Fig. 7, and its corresponding tube surface temperature is 1105 K. On the contrary, the radiation intensity in visible wavelength region (400–600 nm) is apparently low. The black curve in Fig. 7 presents the measured radiation spectrum of the proposed combustor at the tube surface temperature of 1100 K. The main radiation spectrum is congregated similarly in the near-infrared region, but the radiation intensity in the visible range from the combustor is significantly increased compared to that from the silicon carbide tube at the approximately identical surface temperature. It is evident that the radiation from the combustor simultaneously combines the flame

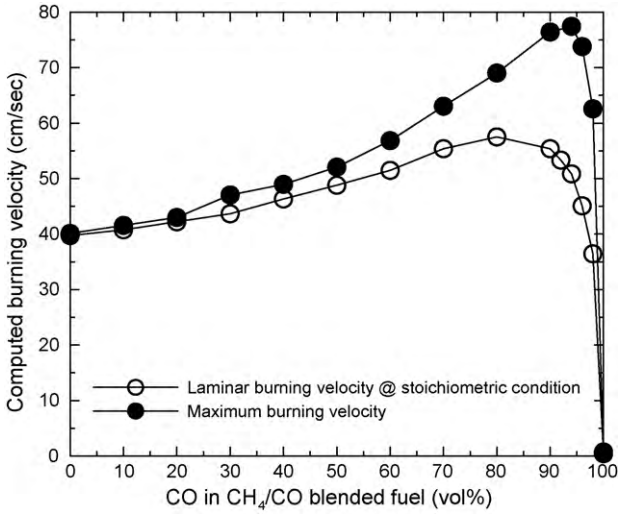

Fig. 5. The computed maximum burning velocity and laminar burning velocity for the stoichiometric CH_4/CO/air flames with various CO contents in the fuel mixture.

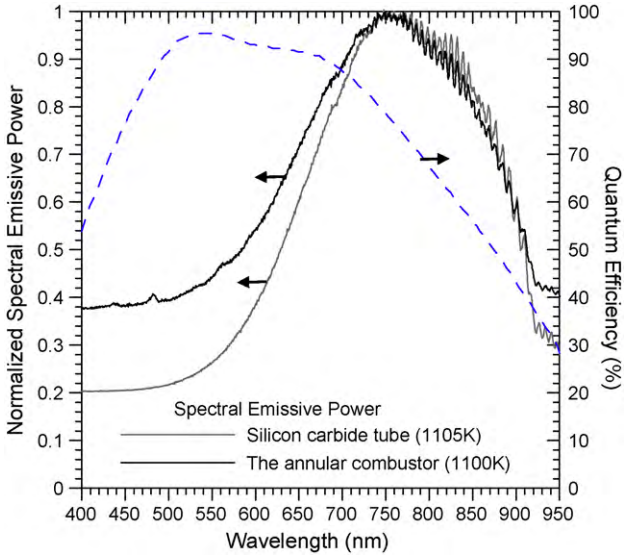

Fig. 7. Spectrum distribution of SiC emitter radiation, and flame luminosity coupling with emitter radiation.

luminosity and emitter radiation, and it proves that the proposed combustor design can successfully superpose the two radiation effects.

As for a new combustor design, proper operational envelopes are important checkpoints to evaluate the performance of the combustor. There are many factors which affect the combustion phenomenon of the combustor. In this study, two essential issues, i.e. fuel composition and emitter diameter, are performed to examine the significance of these parameters on the performance of the proposed combustor design. Stable operation of the combustor defines that the flame can constantly stabilize inside the combustion chamber when operating the combustor. The upper limit of the stable operational envelope is the flame quench due to strong swirling flow, while the low limit of the stable operational envelope is defined by the condition when flame is blown off and burns on the chamber exit. Fig. 8 shows the stable operational envelopes for different fuel compositions, 90%CH_4 + 10%CO, 50%CH_4 + 50%CO and 10%CH_4 + 90%CO respectively. The diameter of the emitter tube is 9 mm and the distance h is 15 mm. Experimental results indicate that the case of 90%CH_4 + 10%CO has narrow stable operational envelope and it cannot survive in high fuel flow rate conditions. It is because that the high methane percentage blended fuel (90%CH_4 + 10%CO) has relatively low laminar burning velocity (42 cm/s at stoichiometric condition), so that the flame is hard to stabilize inside the combustion chamber. Nevertheless, when carbon monoxide percentage is increased to 50% in volume, the laminar burning velocity correspondingly increases to 51 cm/s at stoichiometric condition, and its stable operational envelope becomes larger than that in the case of 90%CH_4 + 10%CO. Most stable operating conditions occur in fuel-rich region corresponding to relatively high laminar burning velocities in that region when CO percentage in the blended fuels is increased, as shown in Fig. 4. As carbon monoxide is increased to 90% in the fuel mixture, the stable operational envelope becomes wider than the other cases in high fuel flow rate conditions, but it becomes narrower in low fuel flow rates. Energy density of the CH_4/CO mixture is related to the fuel composition, such as 90%CH_4 + 10%CO (~45.18 MJ/kg), 50%CH_4 + 50%CO (~25 MJ/kg) and 10%CH_4 + 90%CO (~6.07 MJ/kg) respectively. Increasing carbon monoxide percentage in the blended fuels is inversely proportional to the energy density of the blended fuels. Therefore, more fuel flow rate is needed to resist flame quench for the case of 10%CH_4 + 90%CO. It explains that the flame of high carbon monoxide percentage blended fuel is not stable and cannot exist in a low fuel flow rate condition.

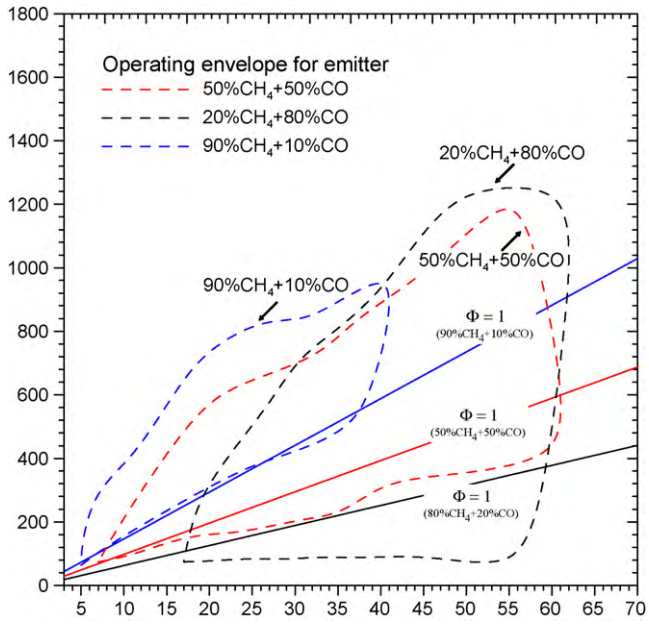

Fig. 8. Stable operating envelopes for the combustor with different fuel compositions.

3.2. Emitter radiant characteristics

To optimize the parameters of the tube diameter D and the distance h for best output performance of the combustor, the powermeter was used to measure radiant intensity in varied fuel compositions. Tables 1 and 2 show the luminous emittance from the combustor at stoichiometric condition and varied fuel compositions. In a high carbon monoxide percentage condition, the flame cannot stably stabilize inside the chamber but anchor on the rim of the combustor exit. No significant illumination can be detected by the powermeter. Depending upon the CO percentage in the CH_4/CO blended fuel mixture, the intensity of the luminous emittance from the combustor is monotonically increasing due to the effect of increasing laminar burning velocity. A large emitter diameter benefits by larger illumination area. However, an increase of emitter diameter means the reduction of the space between combustion chamber and emitter tube for flame. In addition, small space leads to strong swirling flow along the emitter tube, and the flame sheet attaching on the emitter is deteriorated. It explains the fact that flames of 70% and higher carbon monoxide blended fuels can sustain inside the chamber for the case of D = 10 mm, as shown in Table 1. It is observed from Table 1 that when D = 9 mm the current combustor can provide optimal performance in terms of a wider operational range with higher luminous emittance output. On the other hand, the luminous emittance can reach 311.24 W/m^2 for the case of 10%CH_4 + 90%CO when the distance h is further 15 mm, as shown in Table 2. The distance offers a proper space to stabilize the flame. Too small a distance h, say h = 5 mm, would not allow the flame to stabilize on the emitter tube. On the contrary, too large a distance h may reduce the effective illumination area of the emitter tube in the combustion chamber and result in the reduction of the overall luminous emittance. Table 3 shows that the luminous emittance varies with the equivalence ratio at the condition of optimized fuel composition (10%CH_4 + 90%CO). The result reveals that the higher luminous emittance congregates within the fuel-

Table 1
Luminous emittance with different fuel compositions and emitter diameters *D*.

CO in CH_4/CO blended fuel (vol.%)	Luminous emittance (W/m^2) at $h = 15$ mm and $\Phi = 1$		
	$D = 8$ mm	$D = 9$ mm	$D = 10$ mm
0	–	–	–
10	–	185.33	–
30	216.45	219.38	–
50	236.26	261.72	–
70	254.65	292.84	110.35
90	292.84	311.24	91.96

– represents the flame cannot confine inside the chamber.

Table 2
Luminous emittance with different fuel compositions and distance *h*.

CO in CH_4/CO blended fuel (vol.%)	Luminous emittance (W/m^2) at $D = 9$ mm and $\Phi = 1$			
	$h = 5$ mm	$h = 10$ mm	$h = 15$ mm	$h = 20$ mm
0	–	–	–	216.45
10	–	157.03	185.33	222.11
30	–	174.01	209.38	247.57
50	–	179.67	261.72	261.72
70	–	229.18	292.84	268.79
90	–	274.45	311.24	247.57

– represents the flame cannot confine inside the chamber.

Table 3
Luminous emittance functioned with varied equivalence ratio.

Equivalence ratio	Luminous emittance (W/m^2) at $D = 9$ mm and $h = 15$ mm ($10\%CH_4 + 90\%CO$)
0.8	207.96
0.9	240.50
1	311.24
1.2	294.26
1.4	258.89
1.6	210.79
1.8	202.30
2	178.25

rich region (1.0–1.4). The rich shift of maximum laminar burning velocity of the $10\%CH_4 + 90\%CO$ case can applied to elucidate this result.

In order to quantify the uniformity and radiant intensity of illumination on emitter tube, surface temperature along the emitter is measured by IR thermometry. Fig. 9 exhibits the temperature distribution along the emitter for cases of fixed equivalence ratio and flow velocity but with varied fuel compositions. Apparently, for $90\%CH_4 + 10\%CO$ case the emitter has a relatively low surface temperature and its high surface temperature region locates on the top of the emitter tube, indicating the flame anchoring position. Once the CO percentage is increased to 50%, the high surface temperature region and flame anchoring location both move upstream due to enhanced laminar burning velocity. As regards of the $10\%CH_4 + 90\%CO$ case, surface temperature is higher than that of the $50\%CH_4 + 50\%CO$ case. Similarly, the high surface temperature, approximately 1270 K, appears in the bottom of the emitter tube. However, the illumination on the emitter tube is not uniform.

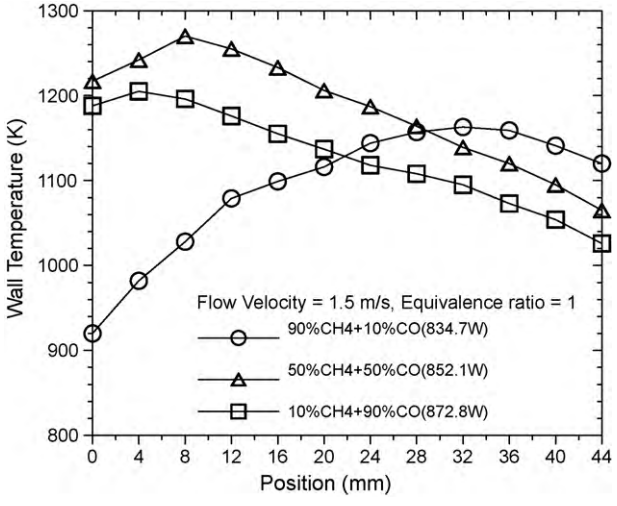

Fig. 9. Measured wall temperature distributions along the axial direction for different fuel compositions.

3.3. Systematic efficiency demonstration

In order to further evaluate the feasibility of using the proposed miniature combustor in a TPV system, GaSb PV cell array was employed to convert illumination emission into electricity output. The electrical power output of the combustor incorporating GaSb cell modules is then measured for various equivalence ratios and different fuel compositions. Table 4 shows the maximum electrical power output for three cases, $20\%CH_4 + 80\%CO$, $50\%CH_4 + 50\%CO$ and $90\%CH_4 + 10\%CO$ respectively. As aforehand description, the electrical output intensity of the TPV power system accounts for the superposed light intensity of flame luminosity and emitter radiation, which is related to the laminar burning

Table 4
The maximum electrical power output under different fuel compositions and equivalence ratios.

Equivalence ratio	Power (W) $20\%CH_4$–$80\%CO$	Power (W) $50\%CH_4$–$50\%CO$	Power (W) $80\%CH_4$–$20\%CO$
0.8	1.15	1.11	0.83
0.9	1.30	1.45	0.26
1	1.45	1.62	0.02
1.2	1.79	0.25	–
1.4	1.35	0.04	–
1.6	1.03	0.02	–
1.8	0.92	–	–
2	0.77	–	–

– represents the flame cannot confine inside the chamber.

velocity of the blended fuels. It is because the flame anchoring position represents a balance between flow velocity and flame burning velocity, and this effect further influences the incandescence feature of the emitter tube. Therefore, the maximum electrical output occurs on fuel-rich side of the equivalence ratio for the case of 20%CH_4 + 80%CO, in stoichiometry for 50%CH_4 + 50%CO, and in fuel-lean for 80%CH_4 + 20%CO. This trend confirms the computed results in Fig. 5. The 80%CH_4 + 20%CO fuel has relatively high energy density, but the flame is rarely stabilized inside the combustion chamber. It turns out that the highest electrical power output for this fuel composition is 0.83 W, while the 20%CH_4 + 80%CO fuel, though has relatively low energy density, has a highest electrical power output of 1.79 W at the equivalence ratio of 1.2. However, further increase in the equivalence ratio in the fuel-rich CH_4/CO flame would diminish the light intensity of visible wavelength in flame luminosity, and result in the reduction of the overall power efficiency of the TPV system. In summary, the idea of integrating flame luminosity and emitter radiation in the proposed novel combustor design by means of combusting CH_4/CO mixtures are demonstrated to be feasible and significantly enhance the output power efficiency of the TPV system.

4. Conclusion

A new concept of a mesoscale high-luminescence flame TPV system is proposed and a novel combustor based upon this concept is designed and tested. High CO concentration percentage blended fuel generates a high-luminescence flame caused by yielding metal oxide particle in flue gas. Superposing flame luminescence and emitter incandescence is expected to enhance the emission ranging from visible to near-infrared wavelength. The experimental results prove the feasibility of the proposed combustor and verify that high CO concentration percentage in the CH_4/CO blended fuel can apparently increase the overall emission intensity of the combustor compared to high methane concentration case. The stable operating of the combustor is strongly related to the fuel compositions, and most stable operation congregates in fuel-rich region due to the shaft of laminar burning velocity in CH_4/CO flame. Besides, the optimum parameter of diameter D and distance h are also tested. Eventually, the maximum electric power output of the combustor assembling with PV cell array is 1.79 W in the stoichiometric 20%CH_4 + 80%CO condition.

Acknowledgment

This work was supported by the National Science Council of the Republic of China under grant number NSC95-2221-E-006-392-MY3 (YCC).

References

[1] D. Dunn-Rankin, E.M. Leal, D.C. Walther, Personal power system, Progress in Energy Combustion Science 31 (2005) 422–465.
[2] L.C. Chia, B. Feng, The development of a micropower (micro-thermophotovoltaic) device, Journal of Power Sources 165 (2007) 455–480.
[3] Y.H. Li, Y.S. Lien, Y.C. Chao, D. Dunn-Rankin, Performance of a mesoscale liquid fuel-film combustion-driven TPV power system, Progress in Photovoltaics: Research and Applications 17 (2009) 327–336.
[4] Y.H. Li, H.Y. Li, D. Dunn-Rankin, Y.C. Chao, Enhancing thermal, electrical efficiencies of a miniature combustion-driven thermophotovoltaic system, Progress in Photovoltaics: Research and Applications 17 (2009) 502–512.
[5] Y.H. Li, Y.C. Chao, Development of a Meso-Scale Central-Porous-Fuel-Inlet Combustor, VDM Verlag Dr. Muller Aktiengesellschaft & Co. KG, 2008.
[6] L.G. Ferguson, L.M. Fraas, Theoretical study of GaSb PV cell efficiency as a function of temperature, Solar Energy Materials & Cell 39 (1995) 11–18.
[7] C.A. Wang, H.K. Choi, S.L. Ransom, G.W. Charache, L.R. Danielson, D.M. DePoy, High-quantum-efficiency 0.5 eV GaInAsSb/GaSb thermophotovoltaic devices, Applied Physics Letters 75 (1999) 1305–1307.
[8] L.G. Ferguson, F. Dogan, A highly efficient NiO-doped MgO matched emitter for thermophotovoltaic energy conversion, Material Science and Engineering B 83 (2001) 35–41.
[9] B. Bitnar, W. Durisch, J.-C. Mayor, H. Sigg, H.R. Tschudi, Characterisation of rare earth selective emitters for thermophotovoltaic application, Solar Energy Materials and Solar Cells 73 (2002) 221–234.
[10] W.M. Yang, S.K. Chou, C. Shu, H. Xue, Z.W. Li, Development of a prototype micro-thermophotovoltaic power generator, Journal of Physics D: Applied Physics 37 (2004) 1017–1020.
[11] C.Y. Wu, Y.C. Chao, T.S. Cheng, C.P. Chen, C.T. Ho, Effects of CO addition on the characteristics of laminar premixed CH_4/air opposed-jet flames, Combustion and Flame 156 (2009) 362–373.
[12] T.C. Williams, C.R. Shaddix, Contamination of carbon monoxide with metal carbonyls: implications for combustion research, Combustion Science and Technology 179 (2007) 1225–1230.
[13] D. Reinelt, G.T. Linteris, Experimental study of the inhibition of premixed and diffusion flames by iron pentacarbonyl, Proceedings of Combustion Institute 26 (1996) 1421–1428.
[14] M.D. Rumminger, G.T. Linteris, The role of particles in the inhibition of counterflow diffusion flames by iron pentacarbonyl, Combustion and Flame 128 (2002) 145–164.
[15] J. Sendroy, H.A. Collinson, H.J. Mark, Determination of iron pentacarbonyl in commercial carbon monoxide, Analytical Chemistry 27 (1955) 1641–1645.
[16] M.H. Wu, Y. Wang, V. Yang, R.A. Yetter, Combustion in meso-scale vortex chambers, Proceedings of the Combustion Institute 31 (2007) 3235–3242.
[17] T.G. Scholte, P.B. Vaags, Burning velocities of mixtures of hydrogen, carbon monoxide and methane with air, Combustion and Flame 3 (1959) 511–524.